

Copyright ©

Es gilt deutsches Urheberrecht.

Die Schrift darf zum eigenen Gebrauch kostenfrei heruntergeladen, konsumiert, gespeichert oder ausgedruckt, aber nicht im Internet bereitgestellt oder an Außenstehende weitergegeben werden ohne die schriftliche Einwilligung des Urheberrechtsinhabers. Es ist nicht gestattet, Kopien oder gedruckte Fassungen der freien Onlineversion zu veräußern.

German copyright law applies.

The work or content may be downloaded, consumed, stored or printed for your own use but it may not be distributed via the internet or passed on to external parties without the formal permission of the copyright holders. It is prohibited to take money for copies or printed versions of the free online version.

On the determination of vertical velocities in the tropical Atlantic Ocean

by

R.-R. WITTSTOCK and G. SIEDLER

Institut für Meereskunde an der Universität Kiel

With 9 figures and 4 tables

Zur Bestimmung von Vertikalgeschwindigkeiten im tropischen Atlantik

Zusammenfassung

Spektren der Vertikalgeschwindigkeit im Meer lassen sich mit drei indirekten Methoden gewinnen: Verfolgung der Verlagerung von Isopyknenflächen, Verfolgung der Verlagerung von Isothermenflächen oder Berechnung der vertikalen Wasserverlagerung aus Temperatur-Zeitreihen für feste Druckniveaus, wobei der mittlere vertikale Temperaturgradient für den Konversionsfaktor herangezogen wird. Diese dritte Methode lässt sich am leichtesten anwenden.

Daten von GATE 1974, die sich aus CTD-Profilmessungen auf F. S. „Meteor“ und aus Temperaturmessungen auf Verankerungen ergaben, werden benutzt, um die Gleichwertigkeit der drei Methoden zu überprüfen. Es wird gezeigt, daß innerhalb der 95%-Vertrauensgrenzen keine signifikanten Abweichungen auftreten; alle drei Methoden sind anwendbar. Dies bedeutet jedoch nicht, daß ebenso eine Gleichwertigkeit der momentanen Meßwerte vorausgesetzt werden kann, denn in Einzelereignissen treten zeitweise wesentliche Abweichungen zwischen den tiefpaßgefilterten Vertikalverlagerungskurven auf. Diese Ereignisse sind offenbar auf die Advektion von anderen Wassermassen zurückzuführen.

Summary

Vertical velocity spectra can be determined by three different indirect methods: Following isopycnal surface displacements, following isothermal surface displacements, or calculating water particle displacements from temperature time series at fixed pressure levels,

with the mean vertical temperature gradient used for the conversion factor. This third method is the easiest to perform.

Data from GATE 1974, obtained by CTD profiling onboard R. V. "Meteor" and by temperature measurements on moorings, are used to check whether the three methods are equivalent. It is shown that auto-spectra do not differ significantly within the 95 % confidence intervals, and either method can be applied. This does not infer an equivalence with respect to the actual data points since individual events were found in the low-passed time series with deviations occurring between displacement curves obtained by the different methods. These events were apparently due to the advection of another water mass.

1. Introduction

The ratio of vertical to horizontal kinetic energy in the ocean is strongly frequency dependent and increases with frequency. While being negligible in the kinetic energy balance at low frequencies, the vertical kinetic energy portion becomes particularly important for high-frequency internal waves (VOORHIS 1968). In the near-surface layers this part of the spectrum may contain a major part of the total kinetic energy of the internal wave field (KÄSE & SIEDLER 1979). A direct determination of vertical velocities has been achieved by using rotating neutrally buoyant floats (ROSSBY, VOORHIS & WEBB 1975), but with the easier access to appropriate data, indirect methods are usually applied to determine velocities.

On the short internal wave time scales between the inertial and the local Brunt-Väisälä frequency, vertical water displacements ζ can be obtained by observing

the vertical displacements of isopycnal surfaces ρ_i :

$$\frac{\partial \zeta(\rho_i)}{\partial t} = \frac{1}{g \bar{\rho}} \frac{\partial p(\rho_i)}{\partial t} \quad (1)$$

where $p(\rho_i)$ = pressure at level of isopycnal ρ_i

g = gravity

$\bar{\rho}$ = mean density above pressure level

$p(\rho_i)$

t = time

For equ. (1) to hold, it must be assumed that horizontal density gradients are sufficiently small to neglect advection. Provided isopycnal mixing and compressibility can be neglected, the density ρ_i is a function of a certain temperature T_i and certain salinity S_i only. In that case, the vertical water displacement can also be obtained by following the respective isothermal or isohaline surfaces. With the determination of temperature being less difficult than that of salinity, the following equations will be used:

$$\frac{\partial \zeta(T_i)}{\partial t} = \frac{1}{g \bar{\rho}} \frac{\partial p(T_i)}{\partial t} \quad (2)$$

Yet another method for the indirect determination of vertical water displacements results from converting temperature time series at fixed depth levels into vertical velocities. If temperature is a conservative property and if fine structure can be neglected (SIEDLER 1974), vertical velocity is given by:

$$\frac{\partial T}{\partial t} + u \frac{\partial T}{\partial x} + v \frac{\partial T}{\partial y} + w \frac{\partial T}{\partial z} = 0 \quad (3)$$

where x, y, z = Cartesian coordinates

u, v, w = Velocity components in x, y, z -direction.

With the horizontal advective terms being neglected, one obtains:

$$\frac{\partial \zeta}{\partial t} = w = - \left(\frac{\partial T}{\partial z} \right)^{-1} \frac{\partial T}{\partial t} \quad (4)$$

The mean vertical temperature gradient $(\frac{\partial T}{\partial z})$ can be used if the changes of the mean vertical temperature gradient are small over the respective displacement range.

It is the aim of this paper to check the validity of the described assumptions by comparing vertical velocities computed with equations (1), (2) or (4). A specific data set from the tropical Atlantic will be used.

2. The data set

In GATE 1974, the Atlantic Tropical Experiment of the Global Atmospheric Research Programme (GARP), a small-scale array of moorings and fixed position ships (Fig. 1), centered half-way between the Cape Verde Islands and the equator, provided an opportunity to collect a data set which can be used to test the various vertical velocity determination methods. In this study the following data will be used:

- (i) CTD profiles obtained at one hour intervals with the Multisonde (KROEBEL 1973) down to 200 dbar on the research vessel "Meteor", moored at $8^{\circ} 30' N, 23^{\circ} 27' W$.
- (ii) Temperature time series from instruments at the two-legged surface mooring F1 at $08^{\circ} 49.9' N, 22^{\circ} 52.6' W$.
- (iii) Temperature time series from instruments at the single-point surface mooring F2 at $08^{\circ} 44.8' N, 23^{\circ} 0.4.2' W$.

Presentation of these data sets have been given by PETERS (1978 a, 1978 b) and KÄSE et al. (1978). The specific series used here are summarized in Table 1, the respective accuracy estimates are listed in Table 2.

The following time series were extracted from the above data sets for the intercomparisons:

Mooring F 1:	$\left(\frac{\partial T}{\partial z} \right)^{-1} T(t)$	for selected ρ_i
"Meteor"	$\left(\frac{\partial T}{\partial z} \right)^{-1} T(t)$	for selected ρ_i
	$p(t)$	for selected T_i
	$p(t)$	for selected ρ_i

The array of ships and moorings was placed close to the Intertropical Convergence Zone. A rather steady Equatorial Counter Current transported the upper layer water towards the north-east, with moorings F2 and F1 being downstream of the research vessel "Meteor". The inertial period was 78.4 hrs at F1 and 81.2 hrs at "Meteor".

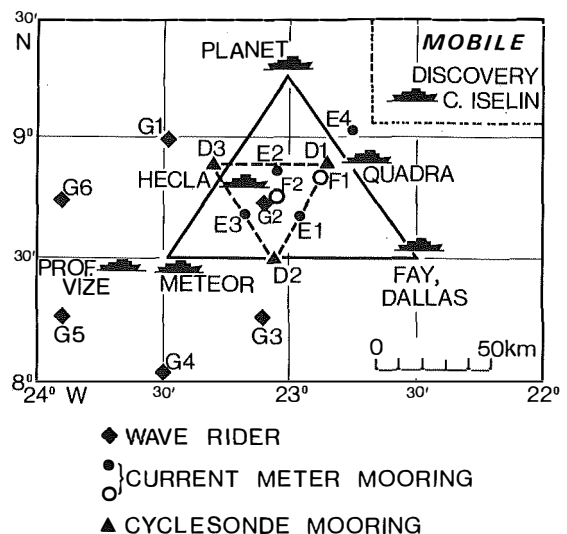


Fig. 1. Ship and mooring positions in the GATE C-Scale Array during Phase III.

Abb. 1. Positionen der Schiffe und Verankerungen im GATE C-Scale-Gebiet während der Meßphase III.

Table 1. Summary of time series used for this study.

Tabelle 1. Übersicht über die für die Untersuchung benutzten Zeitserien.

time (1974)	platform	time series	instruments	sampling rate	averaging interval	number of data points	number of depth levels
30.8., 0.00 h -18.9., 8.45 h	F1	T(t) in P=const	VACM	3.75 Min	o	7437	8
30.8., 0.00 h -18.9., 8.45 h	F1	T(t) in P=const	Bergen	5.0 Min	o	5578	8
30.8., 0.00 h -18.9., 8.45 h	F1	T(t) in P=const	VACM + Bergen	60 Min	o	464	8
30.8., 0.00 h -18.9., 8.45 h	F1	T(t) in P=const	VACM	3.75 Min	60 Min	464	8
30.8., 0.00 h -18.9., 8.45 h	F1	T(t) in P=const	Bergen	5.0 Min	60 Min	464	8
31.8., 0.00 h -11.9., 16.21 h	F2	T(t) in P=const	Bergen	5.0 Min	60 Min	280	5
1.9., 8.00 h -17.9., 12.00 h	FS "Meteor"	T(t) in P=const	Multisonde	60 Min	o	389	5
1.9., 8.00 h -17.9., 12.00 h	FS "Meteor"	P(t) in σ_t =const	Multisonde	60 Min	o	389	5
1.9., 8.00 h -17.9., 12.00 h	FS "Meteor"	P(t) in T=const	Multisonde	60 Min	o	389	5

Table 2. Error estimates.
Tabelle 2. Fehlerschätzwerte.

parameter	accuracy
temperature VACM	$\pm 0.015^\circ \text{C}$
temperature Bergen	$\pm 0.1^\circ \text{C}$
temperature "Multisonde"	$\pm 0.01^\circ \text{C}$
pressure "Multisonde"	$\pm 0.5 \text{ dbar in the range } 0-200 \text{ dbar}$
salinity "Multisonde"	$\pm 0.03 \text{ }^\circ/\text{oo}$
density ρ "Multisonde"	$\pm 2.5 \cdot 10^{-5} \text{ g/cm}^3$

3. Spectral computations

Spectra will mostly be used for the comparisons. With a temperature power spectrum $F_T(\omega)$ as a function of frequency ω , the vertical displacement spectrum $F_\zeta^*(\omega)$ is found from equ. (4):

$$F_\zeta^*(\omega) = \left(\frac{\partial T}{\partial z} \right)^{-2} F_T(\omega) \quad (5)$$

The vertical velocity spectrum $F_w^*(\omega)$ results from differentiating ζ with respect to time:

$$F_w^*(\omega) = \omega^2 F_\zeta^*(\omega) = \omega^2 \left(\frac{\partial T}{\partial z} \right)^{-2} F_T(\omega) \quad (6)$$

Spectra determined by using isoline displacements will be written without a star: $F_w(\omega)$. The vertical kinetic energy except for a factor close to 1, is given by $\frac{1}{2} F_w$. The spectral computations are summarized in Table 3.

The determination of $\left(\frac{\partial T}{\partial z} \right)$ posed a specific problem. Vertical temperature profiles were only available at "Meteor"'s position. A comparison of the mean profile from these CTD-data and of the mean temperature obtained at selected depth levels at mooring F 1 (see Fig. 2) led to the conclusion that the mean vertical gradients were the same at both positions, except for a vertical shift of 3–4 m in the maximum gradient layer.

Due to the different sampling intervals, with 3.75 or 5 minutes at moored instruments and 60 minutes at the CTD, another problem resulted from aliasing. Averaging the moored instrument data over 60 minutes will not lead to spectra that correspond to the spectra obtained from the CTD measurements. This is demonstrated in Fig. 3 with spectra from F 1 data, calculated according to equ. (6). The solid lines

	frequency range [cph]	Mooring F1	CTD "Multisonde"
number of pieces	$\frac{1}{256} \leq \omega \leq \frac{1}{2}$	6, with 50% overlapping	5, with 50% overlapping
	$\frac{1}{32} \leq \omega \leq \frac{1}{2}$	14, without overlapping	12, without overlapping
number of estimates	$\frac{1}{256} \leq \omega \leq \frac{1}{2}$	128	128
	$\frac{1}{32} \leq \omega \leq \frac{1}{2}$	16	16
degrees of freedom	$\frac{1}{256} \leq \omega \leq \frac{1}{2}$	26	22
	$\frac{1}{32} \leq \omega \leq \frac{1}{2}$	61	53
bandwidth of window Hanning	$\frac{1}{256} \leq \omega \leq \frac{1}{2}$	$1.67 \cdot 10^{-2}$ cph	$1.71 \cdot 10^{-2}$ cph
	$\frac{1}{32} \leq \omega \leq \frac{1}{2}$	$6.9 \cdot 10^{-2}$ cph	$6.9 \cdot 10^{-2}$ cph
95% confidence interval	$\frac{1}{256} \leq \omega \leq \frac{1}{2}$	0.62 - 1.8	0.59 - 2.0
	$\frac{1}{32} \leq \omega \leq \frac{1}{2}$	0.72 - 1.4	0.7 - 1.5
sampling rate	$\frac{1}{256} \leq \omega \leq \frac{1}{2}$	1 h	1 h
	$\frac{1}{32} \leq \omega \leq \frac{1}{2}$	1 h	1 h

represent vertical velocity spectra obtained from one-hourly averaged time series, while the broken lines give spectra with data points picked from the original series at one-hour intervals, corresponding to "Meteor"'s CTD data series. Significant deviations occur at frequencies above the semi-diurnal tidal peaks due to aliasing in that case, as is shown in the smoothed high-frequency portion of the spectra given in Fig. 3 b.

4. Comparison of vertical velocity spectra

The frequent CTD profiling on "Meteor" supplied a data set for comparing the three methods corresponding to equations (1), (2) and (4). Five isopycnal surfaces in the pycnocline were selected, and the corresponding isothermal surfaces were computed by averaging temperatures on isopycnals. The corresponding pressure levels resulted from averaging pressure data at these σ_t levels.

$$\begin{aligned}\sigma_t &= \{23.5, 24.0, 24.5, 25.0, 26.0\} \\ T &= \{26.8, 25.6, 23.8, 21.8, 17.4^\circ\text{C}\} \\ p &= \{28, 33, 39, 47, 67 \text{ dbar}\}\end{aligned}$$

The results of the spectral computations are presented in Figs. 4 and 5. The deviations between corre-

sponding spectra are well within the 95 % confidence limit.

Since spectra describe mean statistical properties of the field of motion, it is interesting to check whether there occur events where this equivalence of vertical displacement determinations by the three different methods does not exist. When high-pass filtering the data (limiting frequency: 1 cycle per day), no significant deviations are found. Low-pass filtering leads to the time series presented in Fig. 6. During some periods significant depth variations are found, with a special event on September 12 with a pressure difference $\Delta p = 4.3$ dbar between isopycnal and isothermal surfaces. Contrary to the usual conditions, the vertical salinity profiles at this time (Fig. 7) indicate an increase in the vertical extension of the tropical salinity maximum in the pycnocline. Such a change from profile 0 to 1 can not be caused by internal wave distortion, but will be generated by the advection of high salinity water.

In order to relate data from the Multisonde and from moored temperature sensors, four vertical velocity spectra are combined in Fig. 8. Major deviations occur at the semi-diurnal tidal peak, with the energy being higher by one order of magnitude at the position of mooring F 1. Otherwise, differences are just within the 95 % confidence interval, but with systematically

Table 3. Summary of spectral estimates.

Tabelle 3. Übersicht über die Spektralbeziehungen.

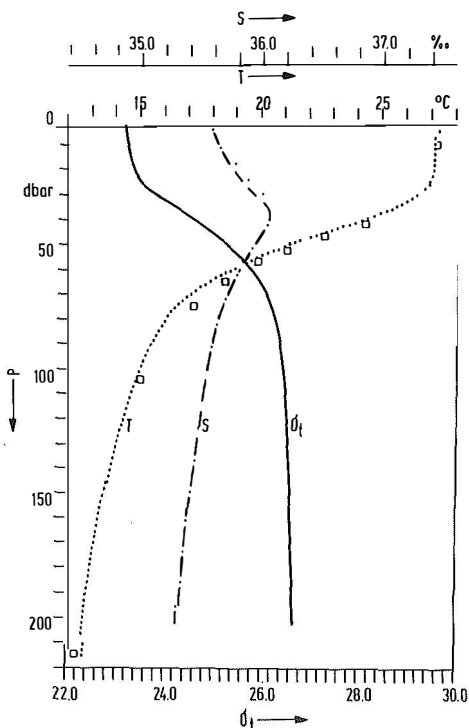


Fig. 2. Mean vertical profiles of temperature T , salinity S and σ_t as a function of pressure p obtained from Multisonde measurements on R. V. "Meteor" during GATE Phase III. The squares indicate mean temperatures from measurements on mooring F 1.

Abb. 2. Mittlere Vertikalprofile der Temperatur T , des Salzgehalts S und von σ_t als Funktion des Drucks p nach Multisondenmessungen von F. S. „Meteor“ während der GATE-Phase III. Die Quadrate geben mittlere Temperaturen nach Messungen der Verankerung F 1 an.

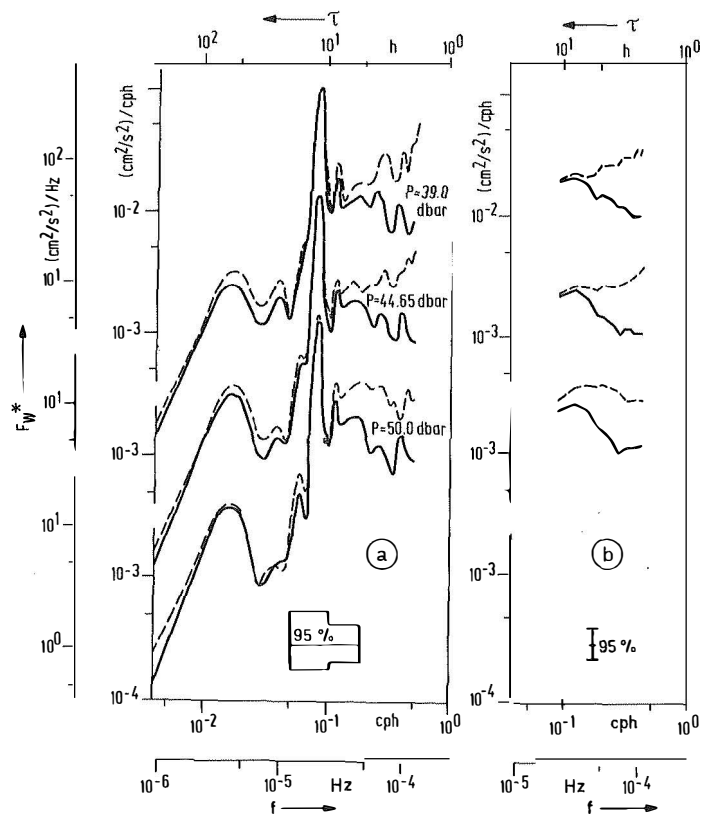


Fig. 3 a. Vertical velocity spectra obtained from mooring F 1 data after one-hourly averaging (solid lines) and after selecting data points at one hour intervals (broken lines) and b) smoothed high-frequency portion of the spectra.

Abb. 3 a. Spektren der Vertikalgeschwindigkeit nach Daten von der Verankerung F 1, einstündig gemittelt (ausgezogene Linien) und nach Auswahl von Meßpunkten mit einstündigem Abstand (gestrichelte Linien) und b) geglättete hochfrequente Teile dieser Spektren.

reduced values at low frequencies for F 1. Although mooring F 1 was positioned downstream of "Meteor", spectral properties thus deviate to some extent at tidal and lower frequencies.

5. Estimation of errors due to advection

The horizontal advection terms of equ. (3) have been neglected throughout this discussion. The temperature data from these three positions ("Meteor", F 1, F 2) and the current data from mooring F 1 provide approximate figures for these advective terms. The following perturbation assumption will be used:

$$\begin{aligned} T &= T^0 + T^1 \\ u &= u^0 + u^1 \text{ (east)} \\ v &= v^0 + v^1 \text{ (north)} \end{aligned}$$

with mean values $\bar{T} = T^0$, $\bar{u} = u^0$ and $\bar{v} = v^0$ resulting when averaged over the total observation period. For the purpose of this order-of-magnitude error estimate, standard deviations from these mean values are taken as perturbation terms, and the maximum typical horizontal gradients are computed from these terms. The results are summarized in Table 4. Using these numbers (see WITTSTOCK 1978) one arrives at an error of approximately 10 % of the vertical velocity determination by using equ. (4), or at an error of approximately 20 % in the spectra. This error interval is considerably smaller than the 95 % confidence intervals.

6. Conclusions

It was shown that auto-spectra of vertical velocity in the internal wave frequency band could be determined

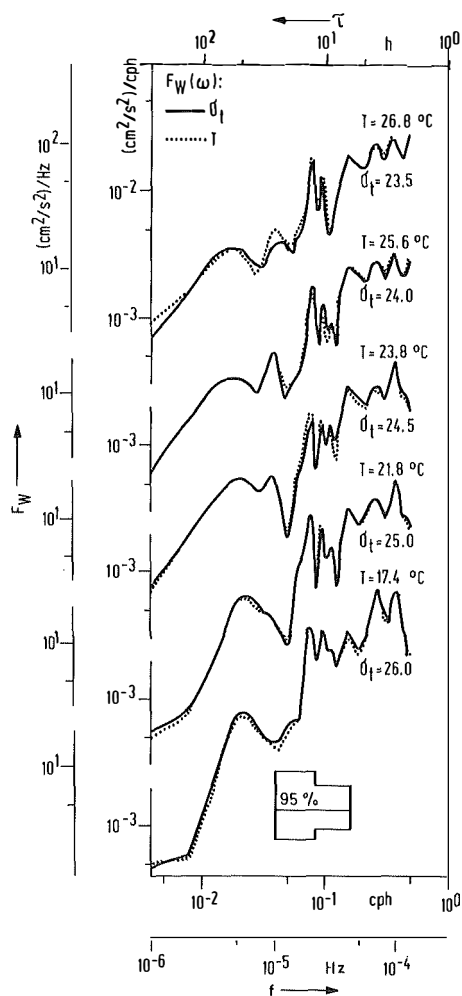


Fig. 4. Vertical velocity spectra obtained from "Meteor" Multisonde profiles by following isothermal surface displacements (dotted lines) and isopycnal surface displacements (solid lines).

Abb. 4. Spektren der Vertikalgeschwindigkeit nach "Meteor"-Multisondeprofilen, berechnet aus Isothermenverlagerungen (gepunktete Linien) und Isopyknenverlagerungen (ausgezogene Linien).

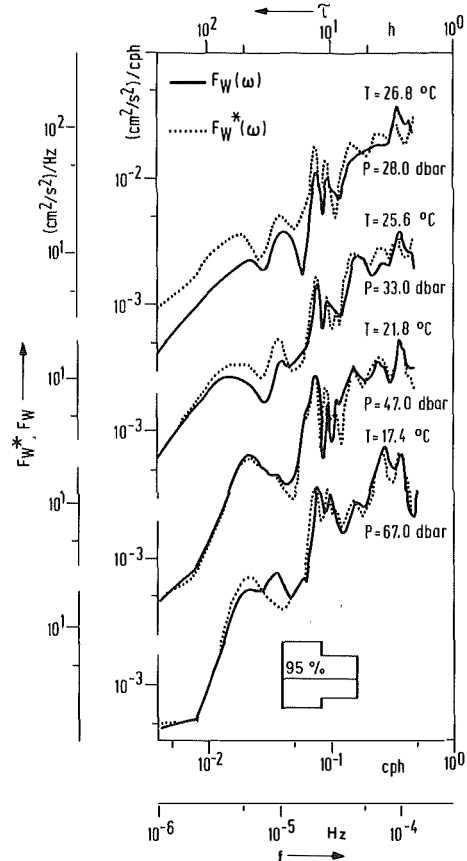


Fig. 5. Vertical velocity spectra obtained from "Meteor" Multisonde profiles by following isothermal surface displacements (solid lines) and from fixed pressure level temperature time series (dotted lines).

Abb. 5. Spektren der Vertikalgeschwindigkeit nach "Meteor"-Multisondeprofilen, berechnet aus Isothermenverlagerungen (ausgezogene Linien) und aus Temperaturzeitreihen auf festen Druckniveaus (gepunktete Linien).

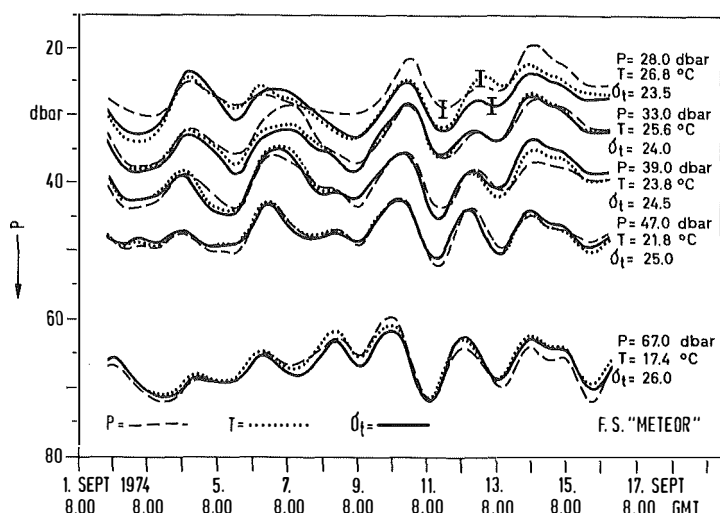


Fig. 6. Vertical displacements of water particles, determined from isothermal (dotted lines) and isopycnal surface displacements (solid lines) and computed from temperature time series at fixed pressure levels (broken lines). Error intervals are indicated.

Abb. 6. Vertikalverlagerungen der Wasserpartikel nach Isothermen- (gepunktete Linien) und Isopyknenverlagerungen (ausgezogene Linien) und nach Berechnungen aus Temperatur-Zeitreihen für feste Druckniveaus (gestrichelte Linien). Fehlerintervalle sind angegeben.

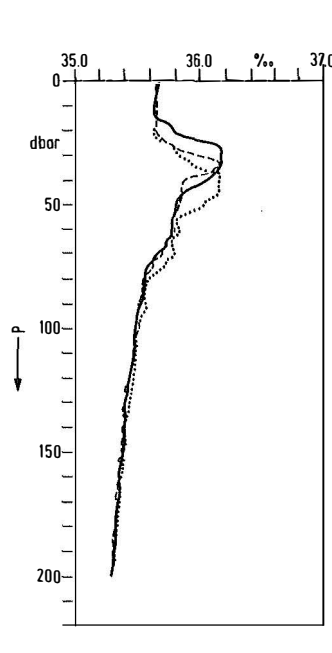


Fig. 7. Salinity profiles obtained from the "Meteor" Multisonde on 13 September, 0.00 h (broken line), 1.00 h (solid line) and 2.00 h (dotted line).

Abb. 7. Salzgehaltsprofile mit der „Meteor“-Multisonde am 13. September, 0.00 Uhr (gestrichelte Linie), 1.00 Uhr (durchgezogene Linie) und 2.00 Uhr (gepunktete Linie).

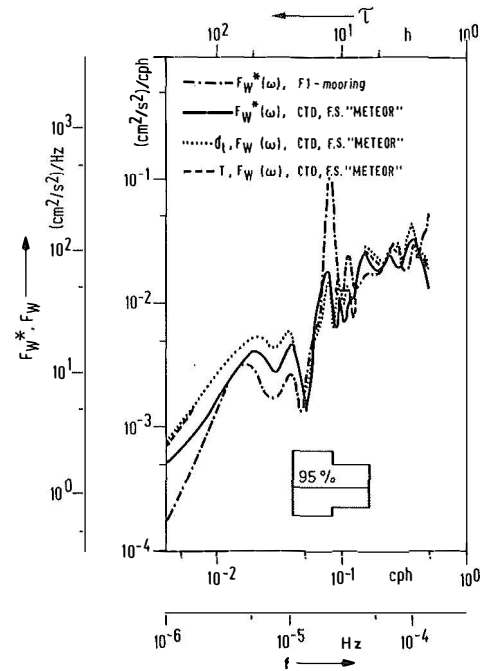


Fig. 8. Vertical velocity spectra obtained by the methods described in the text for R. V. "Meteor" and mooring F 1 at pressure level 39 dbar.

Abb. 8. Spektren der Vertikalgeschwindigkeit nach Berechnungen mit den im Text beschriebenen Methoden für F. S. „Meteor“ und Verankerung F 1 bei einem Druckniveau von 39 dbar.

Table 4. Magnitudes of terms for advection error estimate.

Tabelle 4. Größen der Terme für die Abschätzung des Fehlers infolge Advektion.

term	parameter used		$^{\circ}\text{C} \cdot \text{cm}^{-1}$
$\frac{\Delta T^0}{\Delta t}$	-		$4 \cdot 10^{-6}$
$u^0 \frac{\Delta T^0}{\Delta x}$	$u^0 = 30 \frac{\text{cm}}{\text{sec}}$	$\frac{\Delta T^0}{\Delta x} = 2 \cdot 10^{-7} \frac{{}^{\circ}\text{C}}{\text{cm}}$	$6 \cdot 10^{-6}$
$v^0 \frac{\Delta T^0}{\Delta y}$	$v^0 = 2 \frac{\text{cm}}{\text{sec}}$	$\frac{\Delta T^0}{\Delta y} = 6 \cdot 10^{-7} \frac{{}^{\circ}\text{C}}{\text{cm}}$	$12 \cdot 10^{-7}$
$w^0 \frac{\Delta T^0}{\Delta z}$	$w^0 = 4 \cdot 10^{-3} \frac{\text{cm}}{\text{sec}}$	$\frac{\Delta T^0}{\Delta z} = 3 \cdot 10^{-3} \frac{{}^{\circ}\text{C}}{\text{cm}}$	$12 \cdot 10^{-6}$
$\frac{\Delta T^1}{\Delta t}$	-		$2 \cdot 10^{-4}$
$u^1 \frac{\Delta T^0}{\Delta x}$	$u^1 = 8 \frac{\text{cm}}{\text{sec}}$	$\frac{\Delta T^0}{\Delta x} = 2 \cdot 10^{-7} \frac{{}^{\circ}\text{C}}{\text{cm}}$	$16 \cdot 10^{-7}$
$v^1 \frac{\Delta T^0}{\Delta y}$	$v^1 = 18 \frac{\text{cm}}{\text{sec}}$	$\frac{\Delta T^0}{\Delta y} = 6 \cdot 10^{-7} \frac{{}^{\circ}\text{C}}{\text{cm}}$	$11 \cdot 10^{-6}$
$u^0 \frac{\Delta T^1}{\Delta x}$	$u^0 = 30 \frac{\text{cm}}{\text{sec}}$	$\frac{\Delta T^1}{\Delta x} = 4 \cdot 10^{-7} \frac{{}^{\circ}\text{C}}{\text{cm}}$	$12 \cdot 10^{-6}$
$v^0 \frac{\Delta T^1}{\Delta y}$	$v^0 = 2 \frac{\text{cm}}{\text{sec}}$	$\frac{\Delta T^1}{\Delta y} = 8 \cdot 10^{-7} \frac{{}^{\circ}\text{C}}{\text{cm}}$	$16 \cdot 10^{-7}$
$w^1 \frac{\Delta T^0}{\Delta z}$	$w^1 = 8 \cdot 10^{-2} \frac{\text{cm}}{\text{sec}}$	$\frac{\Delta T^0}{\Delta z} = 3 \cdot 10^{-3} \frac{{}^{\circ}\text{C}}{\text{cm}}$	$24 \cdot 10^{-5}$
$w^0 \frac{\Delta T^1}{\Delta z}$	$w^0 = 4 \cdot 10^{-3} \frac{\text{cm}}{\text{sec}}$	$\frac{\Delta T^1}{\Delta z} = 1 \cdot 10^{-4} \frac{{}^{\circ}\text{C}}{\text{cm}}$	$4 \cdot 10^{-7}$

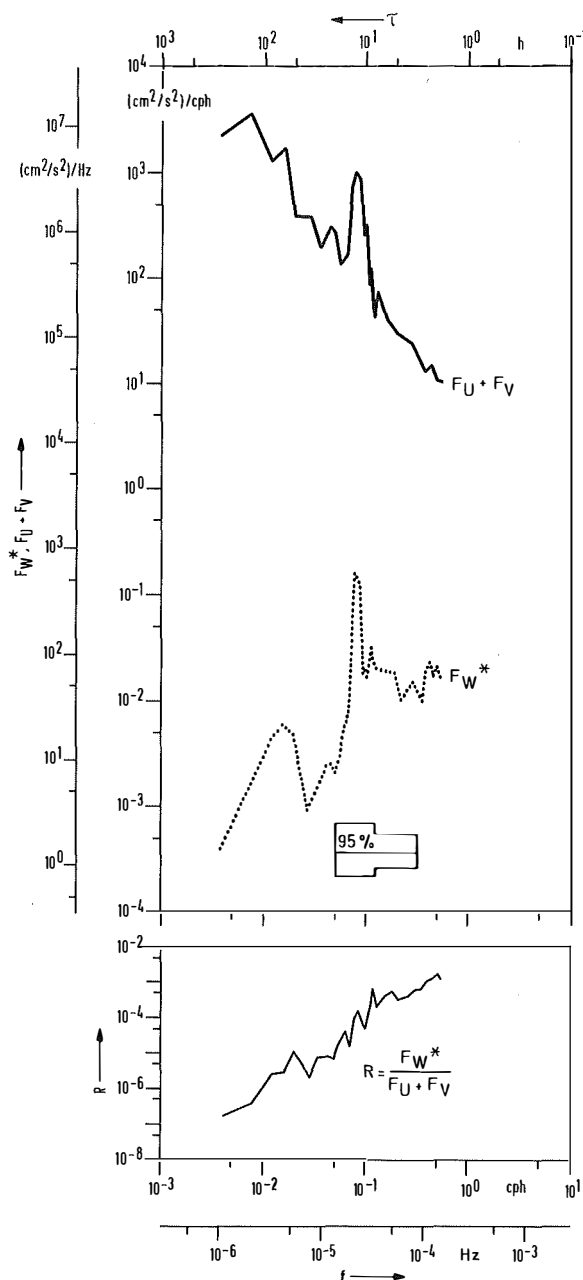


Fig. 9. Horizontal velocity spectrum ($F_u + F_v$), vertical velocity spectrum F_w^* and ratio R of vertical to horizontal kinetic energy.

Abb. 9. Spektrum der Horizontalgeschwindigkeit ($F_u + F_v$), Spektrum der Vertikalgeschwindigkeit F_w^* und Verhältnis R von vertikaler zu horizontaler kinetischer Energie.

by three different methods which proved to be statistically equivalent. It can probably be assumed that this result would also be obtained in other regions and in greater depths. Thus, auto-spectra of vertical velocities can be sufficiently well determined by the simplest method where temperature time series at fixed pressure levels are being used. As an example, the vertical velocity spectrum determined by this method and the horizontal velocity spectrum determined from direct current measurements at mooring F 1 is displayed in Fig. 9, with the ratio R of vertical to horizontal kinetic energy increasing steadily towards higher frequencies.

Acknowledgements

The authors appreciated the assistance of H. PETERS in providing the data base and found the discussion with R. KÄSE particularly helpful. This study was supported by the Deutsche Forschungsgemeinschaft, Bonn-Bad Godesberg.

References

- KÄSE, R. H., PETERS, H., SIEDLER, G. & ZENK, W. (1978): A compilation of current, temperature and conductivity data from moorings F 1 and F 2 in the GATE C-Area. — „Meteo“ Forsch.-Ergebn. A, No. 20: 13—48.
- KÄSE, R. H. & SIEDLER, G. (1979): Internal wave kinematics in the upper tropical Atlantic. — Deep-Sea Res., GATE Suppl. I to Vol. 26 A, 161—189.
- KROEBEL, W. (1973): Die Kieler Multisonde. — „Meteo“ Forsch.-Ergebn. A, No. 12: 53—57.
- PETERS, H. (1978 a): On the variability of the near-surface oceanic layer in the Intertropical Convergence Zone. — Oceanologica Acta 1: 305—314.
- (1978 b): A compilation of CTD- and profiling current meter data from GATE 1974, F. S. „Meteo“ and W. F. S. „Planet“. — „Meteo“ Forsch.-Ergebn. A, No. 20: 49—80.
- ROSSBY, H. T., VOORHIS, A. & WEBB, D. (1975): A quasi-Lagrangian study of mid-ocean variability using long range SOFAR floats. — J. Mar. Res. 33: 355—382.
- SIEDLER, G. (1974): The fine-structure contamination of vertical velocity spectra in the deep ocean. — Deep-Sea Res. 21: 37—46.
- VOORHIS, A. D. (1968): Measurements of vertical motion and the partition of energy in the New England Slope Water. — Deep-Sea Res. 15: 599—608.
- WITRSTOCK, R.-R. (1978): Vergleich der aus Temperatur- und Dichtefluktuationen berechneten Vertikalgeschwindigkeit im GATE-Gebiet. — Ber. Inst. Meeresk. Kiel, 56, 75 pp.

Received 11 October 1979, in revised form 13 December 1979.